

Extra-tropical atmospheric response to ENSO in the CMIP5 models

Margaret M. Hurwitz · Natalia Calvo · Chaim I. Garfinkel ·
Amy H. Butler · Sarah Ineson · Chiara Cagnazzo ·
Elisa Manzini · Cristina Peña-Ortiz

Received: 7 November 2013 / Accepted: 28 February 2014 / Published online: 28 March 2014
© Springer-Verlag Berlin Heidelberg 2014

Abstract The seasonal mean extra-tropical atmospheric response to El Niño/Southern Oscillation (ENSO) is assessed in the historical and pre-industrial control CMIP5 simulations. This analysis considers two types of El Niño events, characterized by positive sea surface temperature (SST) anomalies in either the central equatorial Pacific (CP) or eastern equatorial Pacific (EP), as well as EP and CP La Niña events, characterized by negative SST anomalies in the same two regions. Seasonal mean geopotential height anomalies in key regions typify the magnitude and structure of the disruption of the Walker circulation cell in the tropical Pacific, upper tropospheric ENSO teleconnections and the polar stratospheric response. In the CMIP5 ensembles, the magnitude of the Walker cell disruption is correlated with the strength of the mid-latitude responses in the upper troposphere i.e., the North Pacific and South Pacific lows strengthen during El Niño events. The simulated responses to El Niño and La Niña have opposite sign. The seasonal mean extra-tropical, upper tropospheric responses to EP and

CP events are indistinguishable. The ENSO responses in the MERRA reanalysis lie within the model scatter of the historical simulations. Similar responses are simulated in the pre-industrial and historical CMIP5 simulations. Overall, there is a weak correlation between the strength of the tropical response to ENSO and the strength of the polar stratospheric response. ENSO-related polar stratospheric variability is best simulated in the “high-top” subset of models with a well-resolved stratosphere.

Keywords ENSO · Stratosphere · Teleconnections · CMIP5

1 Introduction

El Niño/Southern Oscillation (ENSO) events contribute to extra-tropical atmospheric variability. Recent literature recognizes two types of El Niño events: eastern Pacific (EP) El

M. M. Hurwitz
Goddard Earth Sciences Technology and Research (GESTAR),
Morgan State University, Baltimore, MD, USA

M. M. Hurwitz (✉)
NASA Goddard Space Flight Center, Code 614, Greenbelt,
MD 20771, USA
e-mail: margaret.m.hurwitz@nasa.gov

N. Calvo
Universidad Complutense de Madrid, Madrid, Spain

C. I. Garfinkel
Hebrew University, Jerusalem, Israel

A. H. Butler
CIRES/NOAA Earth Science Research Laboratory, Boulder,
CO, USA

S. Ineson
Met Office Hadley Centre, Exeter, UK

C. Cagnazzo
Istituto di Fisica dell'Atmosfera e del Clima, Consiglio
Nazionale delle Ricerche (ISAC-CNR), Rome, Italy

E. Manzini
Max Planck Institute for Meteorology, Hamburg, Germany

C. Peña-Ortiz
Universidad Pablo de Olavide, Seville, Spain

Niño and central Pacific (CP) El Niño. These events are characterized by positive sea surface temperature (SST) anomalies in the eastern and central equatorial Pacific, respectively, in boreal autumn and winter (Ashok et al. 2007; Kug et al. 2009).

Meteorological reanalyses and atmospheric simulations forced by observed SSTs show that both types of El Niño modulate the extra-tropical atmosphere. Whereas EP El Niño events do not impact the extra-tropical Southern Hemisphere (SH) stratosphere (e.g., Hurwitz et al. 2011a), CP El Niño events enhance convective activity in the South Pacific Convergence Zone in austral spring, forcing a tropospheric planetary wave that propagates toward SH high latitudes and upward into the Antarctic stratosphere. This wave enhancement affects Antarctic surface temperatures (Schneider et al. 2012) and sea ice concentrations (Song et al. 2011), and leads to anomalously high polar stratospheric temperatures during austral summer (Hurwitz et al. 2011a and Hurwitz et al. 2011b; Zubiaurre and Calvo 2012).

While the NH impacts of EP El Niño events are well established, fewer studies have examined the impacts of CP El Niño events. Manzini et al. (2006), García-Herrera et al. (2006) and Randel et al. (2009), among other studies, have shown that EP El Niño events deepen the North Pacific low and enhance planetary wave driving, leading to a weakening of the Arctic vortex in boreal winter. Garfinkel et al. (2012a) found deepening of the North Pacific low and weakening of the Arctic vortex in late boreal winter, in response to both EP and CP El Niño, in long model simulations. Other analyses of the NH response to CP El Niño (Hegyi and Deng 2011; Xie et al. 2012; Graf and Zanchettin 2012) have found contradictory results, possibly resulting from the dependence of the NH response on the precise definition of CP El Niño and/or the small number of observed events included in these analyses (Garfinkel et al. 2012a). The present multi-model study will support efforts to better understand the NH response to CP El Niño events.

The atmospheric response to La Niña events, characterized by negative SST anomalies in the central and/or eastern equatorial Pacific, is less constrained. La Niña events in the satellite era have had a breadth of locations and magnitudes, and thus it is harder to assess their extra-tropical teleconnections. The available observations suggest that, in the seasonal mean, La Niña events tend to have the opposite atmospheric impacts as El Niño events in the NH, namely a weakening of the North Pacific low (DeWeaver and Nigam, 2002) and a relative strengthening of the Arctic stratospheric vortex (Garfinkel et al. 2012b). Simulations by Zubiaurre and Calvo (2012) indicate that the simulated atmospheric response to CP La Niña is roughly opposite that of CP El Niño. However, Hoerling et al. (1997) and Mitchell et al. (2011) find that, in the NH winter, EP El Niño and La Niña teleconnections are nonlinear. Manzini et al. (2006) find no significant response to La Niña.

In this paper, recent developments in the understanding of the extra-tropical atmospheric response to ENSO, as outlined above, will serve to evaluate interannual atmospheric variability in the Coupled Model Intercomparison, Phase 5 (CMIP5) models (Taylor et al. 2012). The CMIP5 models include an interactive ocean, and are thus capable of simulating ENSO-like variability in the tropical Pacific. The CMIP5 models simulate interannual variability in the central and eastern equatorial Pacific with realistic amplitude (Bellenger et al. 2013), though few models are able to capture strong EP ENSO events (Kim and Yu 2012). More CMIP5 models show a realistic range of ENSO frequencies in the 2–7 year band, in the eastern equatorial Pacific, than for the CMIP3 group of models (Bellenger et al. 2013). SST anomalies peak in November through January, consistent with observations, in approximately half of the CMIP5 models (Bellenger et al. 2013). This is the first multi-model study to consider the responses to two flavors (EP and CP) and both phases (El Niño and La Niña) of ENSO, in both hemispheres. Section 2 introduces the methods, ENSO atmospheric response diagnostics and the meteorological reanalysis dataset used to compare with the CMIP5 models. Section 3 diagnoses the boreal winter response to ENSO in the CMIP5 models. Section 4 summarizes the conclusions and presents a brief discussion.

2 Methods

2.1 Geopotential height diagnostics

In this paper, for simplicity, a single field is used to assess the atmospheric response to ENSO: seasonal mean geopotential height (Z). The tropical diabatic heating anomaly and feedback of the synoptic eddies onto low-frequency variability are left to future work. Geopotential height fields are composited for EP and CP El Niño and La Niña years, following the identification of simulated ENSO events (as in Sect. 2.2) and observed ENSO events (listed in Table 3). Five ENSO diagnostics, based on the geopotential height in specific regions, characterize the extra-tropical atmospheric responses to El Niño and La Niña events (Table 1). Diagnostics measuring Walker circulation disruption (WC), the North Pacific low minimum (NPLM) and the South Pacific low minimum (SPLM) are based on monthly mean Z' (geopotential height deviation from the zonal mean) at 250 hPa. Diagnostics measuring Arctic vortex weakening (NPVW) and Antarctic vortex weakening (SPVW) are based on the monthly and zonal mean polar cap (i.e., 60°–90° latitude) geopotential anomaly at 50 hPa.

WC diagnoses the ENSO response to the difference between Z' in the equatorial eastern Pacific and Z' in the

Table 1 Geopotential height diagnostics

Diagnostic	Definition
Walker circulation disruption (WC)	$Z'(200\text{--}230^\circ\text{E}, 10^\circ\text{S}\text{--}10^\circ\text{N}, 250\text{ hPa})\text{—}$ $Z'(110\text{--}130^\circ\text{E}, 10^\circ\text{S}\text{--}10^\circ\text{N}, 250\text{ hPa})$, NDJF
North Pacific low minimum (NPLM)	$\min[Z'(170\text{--}230^\circ\text{E}, 30\text{--}60^\circ\text{N}, 250\text{ hPa})]$ for El Niño events, DJF $\max[Z'(170\text{--}230^\circ\text{E}, 30\text{--}60^\circ\text{N}, 250\text{ hPa})]$ for La Niña events, DJF
South Pacific low min (SPLM)	$\min[Z'(170\text{--}220^\circ\text{E}, 45\text{--}30^\circ\text{S}, 250\text{ hPa})]$ for El Niño events, OND $\max[Z'(170\text{--}220^\circ\text{E}, 45\text{--}30^\circ\text{S}, 250\text{ hPa})]$ for La Niña events, OND
Arctic vortex weakening (NPVW)	$Z(\text{north of } 59^\circ\text{N}, 50\text{ hPa})$, DJF
Antarctic vortex weakening (SPVW)	$Z(\text{south of } 59^\circ\text{S}, 50\text{ hPa})$, OND

Z' indicates geopotential height deviations from the zonal mean. Means of the NPVW and SPVW regions are weighted with respect to latitude

equatorial western Pacific. Positive values suggest weakened upwelling (i.e., weakened convection and relative downward motion) in the eastern Pacific and enhanced upwelling in the Southeast Asian region. That is, disruption of the zonal Walker Circulation, as expected during El Niño events. Negative values suggest the reverse: a strengthening of the Walker Circulation, as expected during La Niña events. WC measures the change in upper tropospheric divergence associated with El Niño and La Niña events, and thus is a good indicator of the strength of the atmospheric teleconnections. This diagnostic is computed for the NDJF (boreal winter) seasonal mean, coincident with the observed peak in tropical SST anomalies. WC is strongly anti-correlated ($r = -0.81$, for the 1979–2011 period) with an outgoing longwave radiation (OLR) diagnostic based on the NOAA interpolated OLR dataset (Liebmann and Smith 1996), and constructed from differences between the same two regions as for WC. Thus, WC serves as a proxy for the physical tropical atmospheric response to ENSO.

NPLM diagnoses changes in the strength of the North Pacific low. The NPLM is designed such that negative values indicate a deepening of the North Pacific low, as expected during El Niño events (Garfinkel and Hartmann 2008), while positive values indicate a weakening of the North Pacific low, as expected during La Niña events (Garfinkel et al. 2012b). The minimum (maximum) Z' in the Aleutian low region ($170\text{--}230^\circ\text{E}$, $30\text{--}60^\circ\text{N}$), at 250 hPa, is calculated for each El Niño (La Niña) event. Using the minimum (maximum) values of Z' allows the precise location of the North Pacific low to vary between the CMIP5 models. DJF geopotential height anomalies are used to compute the NPLM, since previous studies

(e.g., Garfinkel and Hartmann 2008) have shown that the extra-tropical upper tropospheric response to ENSO is strongest in this season. Note that NPLM yields stronger correlations with WC than does a diagnostic of the average geopotential height anomaly in the Aleutian low region; this result suggests that the precise geographic position of the low varies between models.

SPLM is equivalent to NPLM, but diagnoses changes in the strength of the South Pacific low for the OND seasonal mean. The minimum (maximum) Z' in the region $170\text{--}220^\circ\text{E}$, $45\text{--}30^\circ\text{S}$, at 250 hPa, is calculated for each El Niño (La Niña) event. Atmospheric reanalyses and simulations have shown that the extra-tropical upper tropospheric and stratospheric response to CP ENSO is strongest in austral spring and early summer (Hurwitz et al. 2011a, 2013).

NPVW and SPVW diagnose the polar cap responses to ENSO at 50 hPa. Zonal mean geopotential height at 50 hPa is calculated poleward of 59° latitude in the Arctic (NPVW) and Antarctic (SPVW). Positive values of these diagnostics indicate relative vortex weakening, as expected during El Niño, while negative values indicate vortex strengthening, as expected during La Niña. NPVW is computed for the DJF season, when the observed NH response to ENSO peaks at 50 hPa (Calvo Fernandez et al. 2004; Manzini et al. 2006). Similarly, SPVW is computed for the OND season (Hurwitz et al. 2011a, b, 2013).

2.2 CMIP5 simulations

Two sets of CMIP5 simulations were examined: First, the “historical” simulations of the recent past climate, driven by observed climate forcings (Taylor et al. 2012). The simulated 1951–2005 period was examined, for ease of comparison with meteorological reanalyses. One ensemble member from each of 27 models was included in the analysis. 14 of these models were considered to be “low-top” models (that is, models with lids below the stratosphere and/or few model layers in the stratosphere), while 13 models were considered as “high-top”. Table 2 lists the CMIP5 models included in this analysis. Table 3 lists the range of composite sizes and multi-model mean Niño indices for each type of ENSO event. 100-year subsets of the pre-industrial control (“piControl”) simulations, driven by 1850 climate forcings, from each of 31 models (17 high-top and 14 low-top), provide a second set of simulations (see Tables 2 and 3). The piControl simulations offer larger samples of ENSO events. Comparing two sets of CMIP5 simulations, with different anthropogenic and volcanic prescribed climate forcings, will test if differences in climate conditions affect the atmospheric responses to ENSO.

Four types of ENSO events are examined: EP El Niño, characterized by positive sea surface temperature (SST)

Table 2 Lists of CMIP5 models included in the analysis

Historical	piControl		
CanCM4^a	HadGEM2-AO	ACCESS1-0	GISS-E2-R-CC
CanESM2	HadGEM2-ES	ACCESS1-3	GISS-E2-R
CCSM4	HadCM3	BCC-CSM1-1	HadGEM2-CC
CESM1-WACCM	INMCM4	CanESM2	HadGEM2-ES
CMCC-CESM	IPSL-CM5A-LR	CCSM4	INMCM4
CNRM-CM5	IPSL-CM5A-MR	CESM1-WACCM	IPSL-CM5A-LR
CSIRO-Mk3-6-0	IPSL-CM5B-LR	CMCC-CESM	IPSL-CM5A-MR
FGOALS-G2	MIROC5	CMCC-CMS	IPSL-CM5B-LR
GFDL-CM2.1	MPI-ESM-LR	CNRM-CM5	MIROC5
GFDL-CM3	MRI-CGCM3	CSIRO-MK3-6-0	MPI-ESM-LR
GFDL-ESM2G	NorESM1-ME	FIO-ESM	MPI-ESM-MR
GFDL-ESM2 M		GFDL-CM3	MPI-ESM-P
GISS-E2-H-CC		GFDL-ESM2G	MRI-CGCM3
GISS-E2-H		GFDL-ESM2M	NorESM1-M
GISS-E2-R-CC		GISS-E2-H-CC	NorESM1-ME
GISS-E2-R		GISS-E2-H	

High-top models are highlighted in bold

^a 1961–2005

anomalies in the Niño-3 region (5°S–5°N, 210°–270°E), and CP El Niño, characterized by positive SST anomalies in the Niño-4 region (5°S–5°N, 160°–210°E), as well as EP

and CP La Niña events, characterized by negative SST anomalies in the same two regions. ENSO events are identified based on NDJF seasonal mean SST anomalies, constructed from the monthly mean SST fields provided by the CMIP5 archive. The NDJF season generally corresponds with the observed boreal winter peak in equatorial SST anomalies. SST timeseries are de-trended and computed with respect to the 1979–2000 period (for the historical simulations), and SST anomalies are computed with respect to each 100-year subset (for the piControl simulations). EP El Niño events are identified when the Niño-3 anomaly is both greater than 1 standard deviation above the appropriate mean and 0.1 K larger than the corresponding Niño-4 anomaly. Similarly, EP La Niña events are identified when the Niño-3 anomaly is both less than 1 SD below the climatological mean and 0.1 K less than the Niño-4 anomaly. CP El Niño and CP La Niña events are identified analogously. While Kug and Ham (2011) determined that two distinct types of La Niña events could not be identified from the observational record, the present analysis uses two types of La Niña events for ease of comparison with the response to El Niño events and to highlight similarities between the EP and CP responses. Note that similar results were found when the models with fewer than three events of a particular type in the historical simulations (five events in the piControl simulations) were excluded from the analysis.

2.3 Observational datasets

The Extended Reconstructed Sea Surface Temperature (ERSST) Version 3b dataset (Xue et al. 2003) is used to identify observed ENSO events between 1979 and 2012. Table 3 documents the observed ENSO events included in this analysis and their associated Niño indices; note the small number of events as compared with the CMIP5 multi-model means. No observed events meet the criteria for EP La Niña.

Table 3 Niño index anomalies, numbers of composited events and mean composite size in MERRA and the CMIP5 simulations

		EP El Niño	EP La Niña	CP El Niño	CP La Niña
MERRA	Events composited	1982/1983, 1987/1988, 1997/1998	N/A	1991/1992, 1994/1995, 2002/2003, 2004/2005, 2009/2010	1988/1989, 1998/1999, 1999/2000
	NDJF Niño anomaly	1.86		1.28	−1.59
CMIP5 historical	Events composited	2–8	0–11	2–8	2–12
	Mean composite size	4	4	4	6
	NDJF Niño anomaly	1.72	−1.49	1.44	−1.65
CMIP5 piControl	Events composited	5–21	1–12	2–17	6–14
	Mean composite size	10	6	8	10
	NDJF Niño anomaly	1.68	−1.40	1.38	−1.64

The Niño-3 anomaly is shown for EP cases; the Niño-4 anomaly is shown for CP cases. The range of composite sizes and mean composite sizes are shown for each type of ENSO event

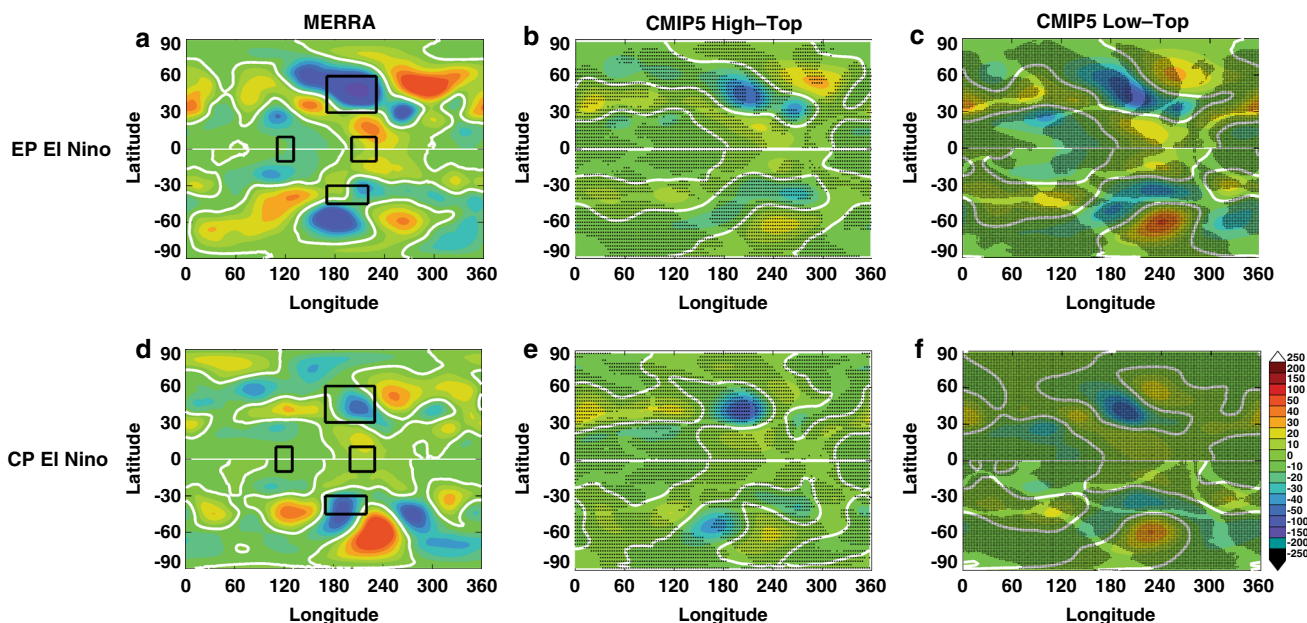


Fig. 1 El Niño teleconnections at 250 hPa in **a, d** MERRA and **b, c, e, f** the CMIP5 historical simulations [m]. In each of the *panels*, the DJF seasonal mean response is shown in the Northern Hemisphere, while the OND seasonal mean response is shown in the Southern

Hemisphere. In **a, d**, *black rectangles* highlight the regions used to calculate the WC, NPLM and SPLM diagnostics. In **b, c, e, f**, *black Xs* indicate regions where at least 80 % of CMIP5 models agree on the sign of the response

Monthly mean geopotential height fields from the Modern-Era Retrospective Analysis for Research and Applications (MERRA) reanalysis (Rienecker et al. 2011) diagnose the observed atmospheric response to ENSO. Data are available from 1979 through 2012. Z anomalies are computed with respect to the 1979–2000 climatological mean.

3 Results

3.1 Upper tropospheric seasonal mean response

On average, the CMIP5 models simulate the observed structure of the seasonal mean ENSO teleconnections at 250 hPa. The multi-model mean, upper tropospheric responses to EP El Niño (upper panels) and CP El Niño (lower panels) are shown in Fig. 1. The teleconnections simulated by the high-top models (center panels) and low-top models (right-hand panels) have weaker amplitudes than those in the MERRA reanalysis (left-hand panels). The relatively weaker multi-model mean responses may be due to the larger number of ENSO events, as compared with the MERRA composite means (e.g., Manzini et al. 2006, their Fig. 4). However, some individual CMIP5 responses are as large or larger than in MERRA. In the tropics, positive height anomalies in the eastern Pacific and negative heights in the western Pacific characterize the Rossby gyres associated with ENSO events (Calvo

Fernandez et al. 2004). Specifically, the anomaly patterns shown in Fig. 1 suggest a disruption of the Walker Circulation in response to both CP and EP El Niño. La Niña events generate height anomaly patterns with the same structure but opposite sign (not shown). Thus, the WC diagnostic is consistently positive in response to both EP and CP El Niño events, in the MERRA reanalysis, historical simulations and piControl simulations. The WC diagnostic is negative during both types of La Niña events (Fig. 2a).

In the extra-tropics, the upper tropospheric responses to El Niño exemplify the Rossby wave responses known as the Pacific-North America (PNA) pattern in the NH and the Pacific-South America-1 (PSA-1) pattern in the SH (Wallace and Gutzler 1981; Mo and Paegle 2001; Calvo Fernandez et al. 2004). These responses are characterized by patterns of upper tropospheric divergence and convergence anomalies that originate in the tropical Pacific, and can be seen in Fig. 1 as alternating patches of positive and negative geopotential height anomalies in the meridional direction, in the Pacific sector. The North Pacific and South Pacific lows strengthen in response to both types of El Niño: mid-latitude height anomalies are negative in the central and western Pacific region (Fig. 1). Correspondingly, both NPLM and SPLM are negative in response to EP and CP El Niño, in MERRA and in both sets of CMIP5 simulations (Figs. 2b, c). NPLM and SPLM are positive in response to both types of La Niña events.

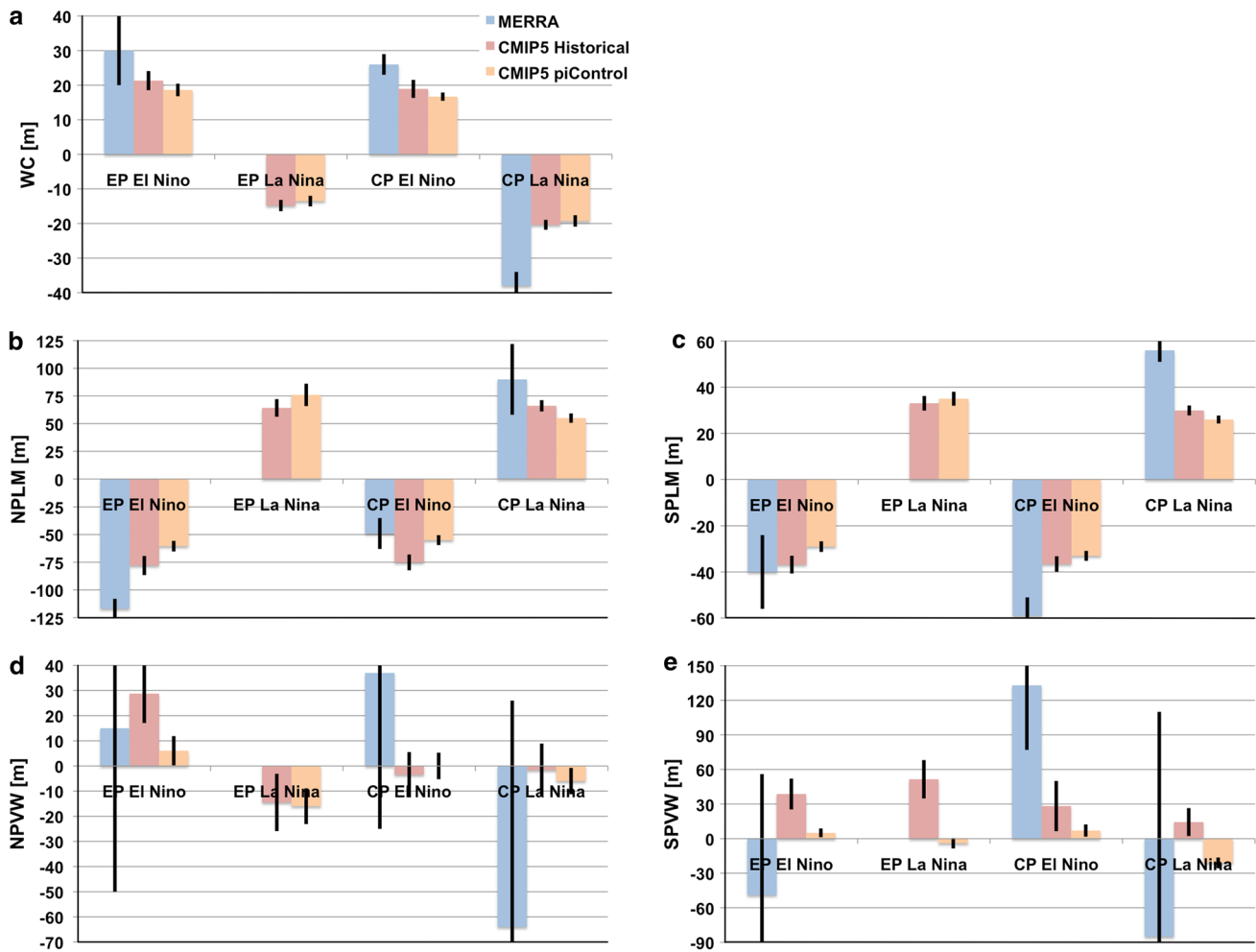


Fig. 2 Geopotential height diagnostics in MERRA and the CMIP5 simulations [m]. *Black error bars* indicate 1 SE

Inter-model variability in the magnitude of the North Pacific and South Pacific low responses is strongly correlated with inter-model variability in the magnitude of the upper tropospheric response to ENSO. Figure 3 shows scatter plots of the WC diagnostic with the NPLM (Fig. 3a) and SPLM (Fig. 3b). The WC diagnostic is strongly anti-correlated with NPLM (and SPLM), for both phases of ENSO. That is, on average, the more positive the tropical Pacific ENSO height anomaly, the more negative the height anomaly in the extra-tropical Pacific (i.e., as expected for the PNA and PSA patterns). The MERRA composite means generally fall within the CMIP5 model scatter. Note that the EP and CP seasonal mean responses are statistically indistinguishable at the 95 % level, in two-tailed t-tests; also note the proximity of the EP and CP multi-model means (symbols with black outlines), for both El Niño and La Niña events and in both hemispheres. The correlations between WC, NPLM and SPLM are quantified in Table 4. The correlations are statistically significant, for both high- and

low-top models, and for all four categories of ENSO events, with only two exceptions. Note that the piControl simulations yield similar results (e.g., for NPLM and WC; see Fig. 5a).

3.2 Polar stratospheric seasonal mean response

As discussed in Sect. 1, previous observational and single-model studies have shown that CP El Niño events tend to weaken the polar vortices while CP La Niña events strengthen the polar vortices. EP El Niño events tend to weaken the Arctic stratospheric vortex and have a negligible impact on the Antarctic vortex. While the MERRA reanalysis demonstrates the sign of these expected responses, likely the responses are not statistically robust because of the small composite size (Table 3). The present CMIP5 study will test the robustness of these previous results.

In the Arctic stratosphere, the historical, multi-model mean responses to ENSO have the expected sign (Fig. 2d).

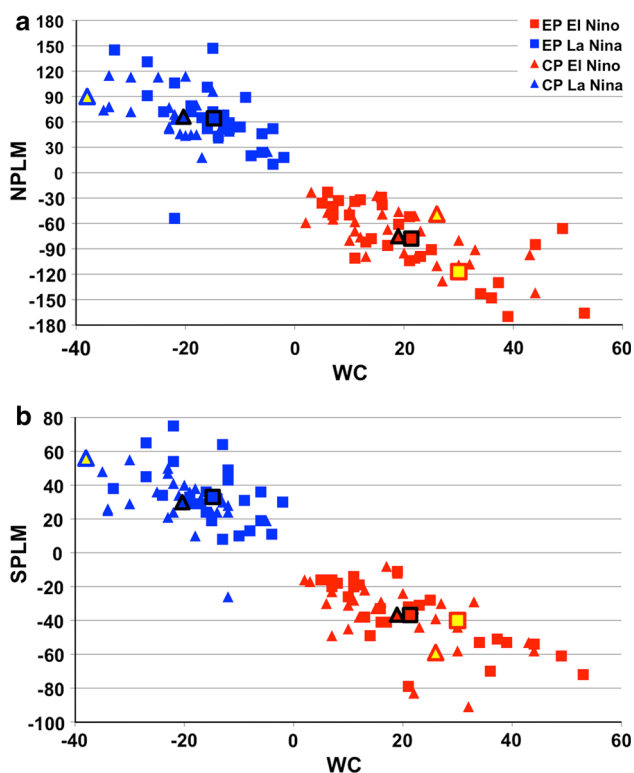


Fig. 3 a NPLM and b SPLM diagnostics [m] with respect to the WC diagnostic, in the CMIP5 historical simulations. *Squares* indicate the response to EP El Niño/La Niña; *triangles* indicate the response to CP El Niño/La Niña. *Red shapes* indicate the response to El Niño; *blue shapes* indicate the response to La Niña. Shapes with *black outlines* indicate the multi-model means. *Yellow shapes* indicate the MERRA reanalysis composite means

The CMIP5 responses are weaker than observed, with the exception of EP El Niño. Figure 4b compares the inter-model variability in WC to that of the Arctic vortex weakening (NPVW). There is more inter-model variability in the Arctic vortex response as compared with the tropospheric responses to ENSO; only for EP El Niño events is the magnitude of the Walker Circulation anomaly significantly correlated with the DJF seasonal mean Arctic vortex weakening (Table 4).

The simulated Antarctic stratospheric responses to ENSO are weaker than in MERRA and only some have the expected sign (Fig. 2e). Figure 4b shows that the magnitude of the Walker Circulation anomaly is not related to the simulated Antarctic vortex weakening.

Weak or negligible multi-model mean responses in the polar stratosphere may reflect the poor performance of the low-top models. Charlton-Perez et al. (2013) found that the CMIP5 low-top models poorly represent stratospheric variability, even though they are able to reproduce observed climate trends. Separating the high-top and low-top models, it emerges that the Arctic response to ENSO is correlated with WC and stronger in the high-top models

Table 4 Correlations between geopotential height diagnostics in the CMIP5 historical simulations

Diagnostics correlated		EP El Niño	EP La Niña	CP El Niño	CP La Niña
High-top Models	WC and NPLM	-0.90	-0.72	-0.57	-0.78
	WC and SPLM	-0.81	-0.55		-0.60
	NPLM and NPVW	-0.80			
	WC and NPVW	0.69			
Low-top Models	SPLM and SPVW				
	WC and SPVW			0.50	
	WC and NPLM	-0.70	-0.48	-0.81	-0.49
	WC and SPLM	-0.71	-0.56	-0.67	
	NPLM and NPVW				
	WC and NPVW				
SPLM and SPVW				-0.46	
WC and SPVW					

Correlation coefficients are based on the composite mean diagnostics for each CMIP5 model. Correlations involving polar stratospheric diagnostics are indicated in bold. Values greater or equal to 0.45, statistically significant at approximately the 95 % confidence level, are shown

(Fig. 4a). Gray shading in Table 4 indicates the correlations with either NPVW or SPVW. In the low-top models, correlations are weak for all types of ENSO events (except for WC vs. NPVW for EP La Niña). In the high-top models, there are significant correlations with e.g., NPVW for EP El Niño, and with SPVW for CP El Niño, in agreement with previous single-model studies. Correlations between WC and the polar vortex weakening diagnostics are similar in the piControl simulations (e.g., for NPVW; see Fig. 5b).

4 Conclusions and discussion

The CMIP5 models simulate the expected upper tropospheric responses to ENSO in boreal autumn and winter. El Niño events disrupt the zonal Walker circulation cell, leading to increased upper tropospheric geopotential heights in the eastern tropical Pacific but decreased heights in the western tropical Pacific. The CMIP5 models generate upper tropospheric wavetrains in response to ENSO. In the

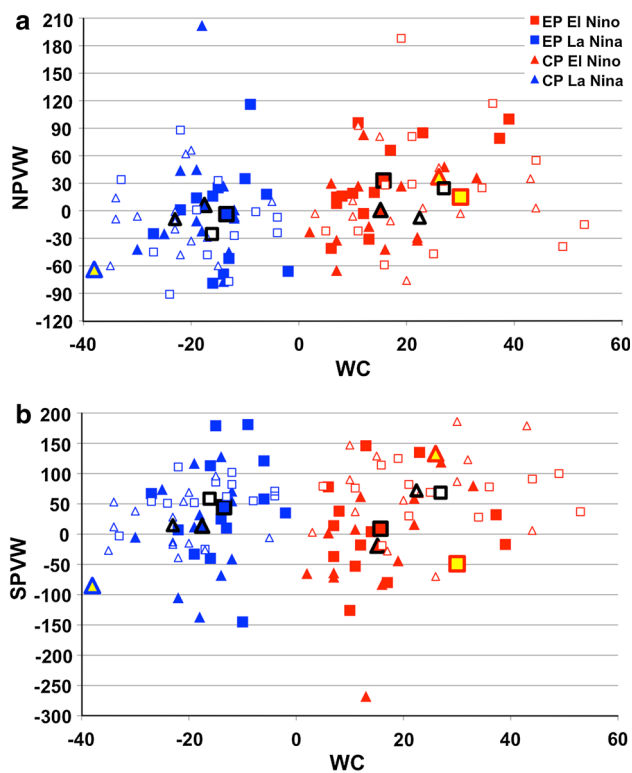


Fig. 4 As for Fig. 3, but for **a** NPVW and **b** SPVW diagnostics [m]. *Hollow red and blue shapes* indicate low-top CMIP5 models; *filled red and blue shapes* indicate high-top CMIP5 models

historical simulations, the structure of these wavetrains is consistent with the MERRA reanalysis composites of ENSO events in the satellite era. On average, El Niño and La Niña events generate the opposite seasonal mean, extratropical atmospheric responses. For example, the mid-latitude North Pacific and South Pacific lows deepen during El Niño events, but weaken during La Niña events. Consistent with the realistic simulation of the North Pacific low response to ENSO, Polade et al. (2013) find the North Pacific teleconnections that link an ENSO–PDO mode with North American winter precipitation are well captured in the CMIP5 models.

In the Arctic stratosphere, observations suggest that the wintertime polar vortex should weaken in response to El Niño events and strengthen in response to La Niña events. The CMIP5 historical and piControl multi-model means do show a vortex weakening during both types of El Niño events and vortex strengthening during both types of La Niña events, in boreal winter, but generally with weaker magnitudes than for the MERRA reanalysis. Furthermore, in the CMIP5 models, there are more strong correlations between the upper tropospheric responses to ENSO and the polar stratospheric responses in the high-top models (i.e., those with a well-resolved stratosphere) than in the low-top models, consistent with Charlton-Perez et al. (2013).

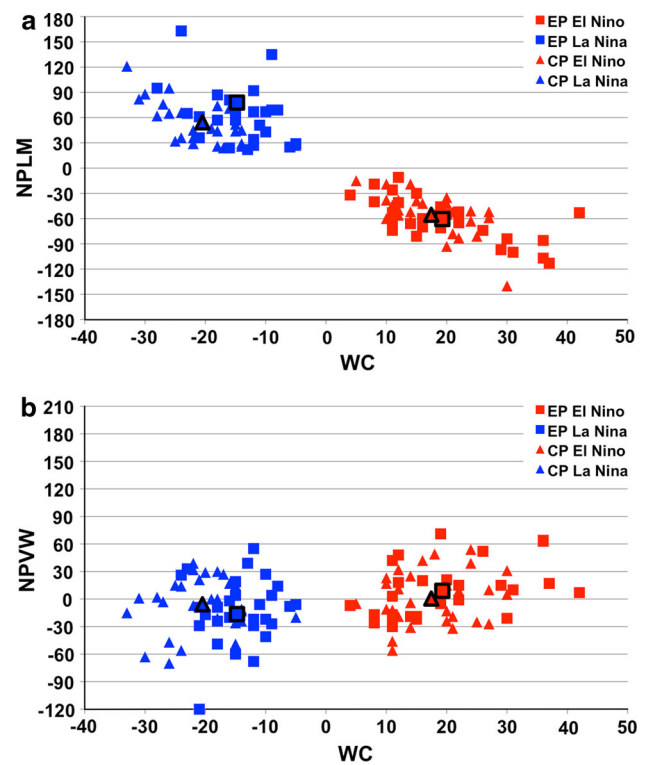


Fig. 5 **a** As for Fig. 3a and **b** as for Fig. 4a, but for the CMIP5 piControl simulations. High- and low-top models are not separated, so as to emphasise the overall multi-model mean correlations between ENSO diagnostics

In the Antarctic stratosphere, most CMIP5 models fail to capture the observed weakening of the polar vortex in response to CP El Niño events. This result reflects a weak poleward planetary wave response in the CMIP5 models, which in turn reflects a weak SPCZ convective response to CP El Niño. Brown et al. (2013) found that the southeastern “diagonal” portion of the SPCZ is poorly represented in the CMIP5 models: the SPCZ precipitation signature is both too zonal and confined to the deep tropics. The GEOSCCM captures the expected stratospheric response to CP El Niño when forced by observed SSTs (Hurwitz et al. 2011b), but fails to capture this response when forced by SSTs from CCSM3, one of the CMIP3 models with a tropically confined SPCZ (Hurwitz et al. 2013). Thus, it is expected that better simulation of the SPCZ, and its full response to ENSO, would improve the simulation of ENSO teleconnections in the SH.

The CMIP5 atmospheric responses to EP and CP ENSO flavors are indistinguishable. In the NH, this result is consistent with the single model study by Garfinkel et al. (2012a). However, in the SH, a strong poleward wavetrain and vortex weakening have been shown to occur only during CP-type El Niño events, both in observations and in model studies (Hurwitz et al. 2011a, b; Zubiaurre and Calvo 2012). The CMIP5 models’ failure to capture two

distinct boreal winter mean responses to El Niño in the SH may occur because these models (1) fail to capture the convective response to CP El Niño in the SPCZ region, as discussed above, and (2) are not able to simulate two distinct ENSO modes. Only 9 of the 20 CMIP5 models investigated by Kim and Yu (2012) were able to simulate both the EP and CP ENSO modes with realistic amplitudes. Kug et al. (2012) found that only 5 of 21 CMIP5 models simulated the observed negative correlation between SST variability in the Niño-3 and Niño-4 regions.

The magnitudes of the equatorial SST anomalies associated with ENSO events are similar in the CMIP5 historical and pre-industrial simulations, as are the resulting extra-tropical atmospheric responses to these events. The structure and magnitude of the seasonal mean, upper tropospheric teleconnections in the piControl simulations (Fig. 5) are similar to those in the historical simulations (Figs. 1, 3, 4). That is, the large difference in climate forcings between the two sets of simulations does not affect the essence of the ENSO teleconnections. This conclusion is consistent with Hurwitz et al. (2013), who compared the atmospheric response to CP El Niño under contemporary and late twenty-first century climate conditions.

Detecting robust stratospheric responses to ENSO requires composites of at least 20 El Niño or La Niña events (Garfinkel et al. 2012a). The small number of events observed during the satellite era limits confidence in the atmospheric responses in MERRA; however, the signs of the responses in this analysis agree with studies with larger sample sizes (e.g., modeling studies by Hurwitz et al. 2011b; Zubiaurre and Calvo 2012; Garfinkel et al. 2012a). While individual historical simulations had composites as small as 2 events (1 event in the piControl simulations; see Table 3), the multi-model means included many dozens of events (i.e., 4–10 events per model \times 30 models), and thus represent a large enough sample to detect robust stratospheric signals.

Acknowledgments Margaret M. Hurwitz thanks the NASA Atmospheric Composition, Modeling and Analysis Program (ACMAP) and Modeling, Analysis and Prediction (MAP) program for funding, and the World Climate Research Programme (WCRP) and Stratospheric Processes and their Role in Climate (SPARC) DynVar for travel support. Sarah Ineson was supported by the Joint DECC/Defra Met Office Hadley Centre Climate Programme (GA01101). The authors thank two anonymous reviewers for their helpful feedback.

References

- Ashok K, Behera SK, Rao SA, Weng H, Yamagata T (2007) El Niño Modoki and its possible teleconnections. *J Geophys Res* 112:C11007. doi:10.1029/2006JC003798
- Bellenger H, Guilyardi E, Leloup J, Lengaigne M, Vialard J (2013) ENSO representation in climate models: from CMIP3 to CMIP5. *Clim Dyn*. doi:10.1007/s00382-013-1783-z
- Brown JR, Moise AF, Colman RA (2013) The South Pacific convergence zone in CMIP5 simulations of historical and future climate. *Clim Dyn* 41:2179–2197. doi:10.1007/s00382-012-1591-x
- Calvo Fernandez N, Garcia RR, Garcia Herrera R, Gallego Puyol D, Gimeno Presa L, Hernandez Martin E, Ribera Rodriguez P (2004) Analysis of the ENSO signal in tropospheric and stratospheric temperatures observed by MSU, 1979–2000. *J Climate* 17:3934–3946
- Charlton-Perez AJ et al (2013) On the lack of stratospheric dynamical variability in low-top versions of the CMIP5 models. *J Geophys Res* 118:2494. doi:10.1002/jgrd.50125
- DeWeaver E, Nigam S (2002) Linearity in ENSO's atmospheric response. *J Climate* 15:2446–2461
- García-Herrera R, Calvo N, García RR, Giorgetta MA (2006) Propagation of ENSO temperature signals into the middle atmosphere: a comparison of two general circulation models and ERA-40 reanalysis data. *J Geophys Res* 111:D06101. doi:10.1029/2005JD006061
- Garfinkel CI, Hartmann DL (2008) Different ENSO teleconnections and their effects on the stratospheric polar vortex. *J Geophys Res* 113:D18114. doi:10.1029/2008JD009920
- Garfinkel CI, Hurwitz MM, Waugh DW, Butler AH (2012a) Are the teleconnections of Central Pacific and Eastern Pacific El Niño distinct in boreal wintertime? *Clim Dyn*. doi:10.1007/s00382-012-1570-2
- Garfinkel CI, Butler AH, Waugh DW, Hurwitz MM, Polvani LM (2012b) Why might stratospheric sudden warmings occur with similar frequency in El Niño and La Niña winters? *J Geophys Res* 117:D19106. doi:10.1029/2012JD017777
- Graf H, Zanchettin D (2012) Central Pacific El Niño, the subtropical bridge, and Eurasian climate. *J Geophys Res* 117:D01102. doi:10.1029/2011JD016493
- Hegyi BM, Deng Y (2011) A dynamical fingerprint of tropical Pacific sea surface temperatures on the decadal-scale variability of cool-season Arctic precipitation. *J Geophys Res* 116:D20. doi:10.1029/2011JD016001
- Hoerling MP, Kumar A, Zhong M (1997) El Niño, La Niña, and the nonlinearity of their teleconnections. *J Climate* 10:1769–1786
- Hurwitz MM, Newman PA, Oman LD, Molod AM (2011a) Response of the Antarctic stratosphere to two types of El Niño events. *J Atmos Sci* 68:812–822. doi:10.1175/2011JAS3606.1
- Hurwitz MM, Song I-S, Oman LD, Newman PA, Molod AM, Frith SM, Nielsen JE (2011b) Response of the Antarctic stratosphere to warm pool El Niño events in the GEOS CCM. *Atmos Chem Phys* 11:9659–9669. doi:10.5194/acp-11-9659-2011
- Hurwitz MM, Garfinkel CI, Newman PA, Oman LD (2013) Sensitivity of the atmospheric response to warm pool El Niño events to modeled SSTs and future climate forcings. *J Geophys Res* 118:13. doi:10.1002/2013JD021051
- Kim ST, Yu J-Y (2012) The two types of ENSO in CMIP5 models. *Geophys Res Lett* 39:L11704. doi:10.1029/2012GL052006
- Kug J-S, Ham Y-G (2011) Are there two types of La Niña? *Geophys Res Lett* 38:L16704. doi:10.1029/2011GL048237
- Kug J-S, Jin F-F, An S-I (2009) Two types of El Niño events: cold tongue El Niño and warm pool El Niño. *J Climate* 22:1499–1515
- Kug J-S, Ham Y-G, Lee J-Y, Jin F-F (2012) Improved simulation of two types of El Niño in CMIP5 models. *Environ Res Lett* 7:034002. doi:10.1088/1748-9326/7/3/034002
- Liebmann B, Smith CA (1996) Description of a complete (interpolated) outgoing longwave radiation dataset. *B Am Meteorol Soc* 77:1275–1277
- Manzini E, Giorgetta MA, Esch M, Kornblüeh L, Roeckner E (2006) The influence of sea surface temperatures on the Northern winter stratosphere: ensemble simulations with the MAECHAM5 model. *J Climate* 19:3863–3881

- Mitchell DM, Gray LJ, Charlton-Perez AJ (2011) The structure and evolution of the stratospheric vortex in response to natural forcings. *J Geophys Res* 116:D15110. doi:[10.1029/2011JD015788](https://doi.org/10.1029/2011JD015788)
- Mo KC, Paegle JN (2001) The Pacific-South American modes and their downstream effects. *International J Climatology* 21:1211–1229. doi:[10.1002/joc.685](https://doi.org/10.1002/joc.685)
- Polade SD, Gershunov A, Cayan DR, Dettinger MD, Pierce DW (2013) Natural climate variability and teleconnections to precipitation over the Pacific-North American region in CMIP3 and CMIP5 models. *Geophys Res Lett* 40:2296. doi:[10.1002/grl.50491](https://doi.org/10.1002/grl.50491)
- Randel WJ, Garcia R, Calvo N, Marsh D (2009) ENSO influence on zonal mean temperature and ozone in the tropical lower stratosphere. *Geophys Res Lett* 36:L15822. doi:[10.1029/2009GL039343](https://doi.org/10.1029/2009GL039343)
- Rienecker MM et al (2011) MERRA—NASA’s modern-era retrospective analysis for research and applications. *J Climate* 24:3624–3648. doi:[10.1175/JCLI-D-11-00015.1](https://doi.org/10.1175/JCLI-D-11-00015.1)
- Schneider DP, Okumura Y, Deser C (2012) Observed Antarctic interannual climate variability and tropical linkages. *J Climate* 25:4048–4066. doi:[10.1175/JCLI-D-11-00273.1](https://doi.org/10.1175/JCLI-D-11-00273.1)
- Song H-J, Choi E, Lim G-H, Kim YH, Kug J-S, Yeh S-W (2011) The central Pacific as the export region of the El Niño-Southern oscillation sea surface temperature anomaly to Antarctic sea ice. *J Geophys Res* 116:D21112. doi:[10.1029/2011JD015645](https://doi.org/10.1029/2011JD015645)
- Taylor KE, Stouffer RJ, Meehl GA (2012) An overview of CMIP5 and the experimental design. *Bull Am Met Soc* 93:485–498. doi:[10.1175/BAMS-D-11-00094.1](https://doi.org/10.1175/BAMS-D-11-00094.1)
- Wallace JM, Gutzler DS (1981) Teleconnections in the geopotential height field during the Northern Hemisphere winter. *Mon Wea Rev* 109:784–812
- Xie F, Li JP, Tian WS, Feng J (2012) Signals of El Niño Modoki in the tropical tropopause layer and stratosphere. *Atm Chem Phys* 12:5259. doi:[10.5194/acp-12-5259-2012](https://doi.org/10.5194/acp-12-5259-2012)
- Xue Y, Smith TM, Reynolds RW (2003) Interdecadal changes of 30-yr SST normals during 1871–2000. *J Climate* 16:1601–1612
- Zubiaurre I, Calvo N (2012) The El Niño-Southern Oscillation (ENSO) Modoki signal in the stratosphere. *J Geophys Res* 117:D04104. doi:[10.1029/2011JD016690](https://doi.org/10.1029/2011JD016690)